

OPEN ACCESS

## Higher Tamm-Dankoff approximation for rotational nuclear states

To cite this article: H Laftchiev *et al* 2010 *J. Phys.: Conf. Ser.* **205** 012005

View the [article online](#) for updates and enhancements.

### You may also like

- [\(Digital Presentation\) Activating the Ion Transmission at the Cathode-Electrolyte Interface in All-Solid-State Batteries](#)  
Yuxuan Zhang, Thomas Kivevele, Han Wook Song et al.
- [ABOUT EXOBIOLOGY: THE CASE FOR DWARF K STARS](#)  
M. Cuntz and E. F. Guinan
- [Determination of a pairing residual interaction from Bohr quadrupole collective dynamics](#)  
M Rebhaoui, M Imadalou, D E Medjadi et al.



**ECS**  
The  
Electrochemical  
Society  
Advancing solid state &  
electrochemical science & technology

**DISCOVER**  
how sustainability  
intersects with  
electrochemistry & solid  
state science research

# Higher Tamm-Dankoff approximation for rotational nuclear states

H Laftchiev<sup>1</sup>, J Libert<sup>2</sup>, P Quentin<sup>3</sup> and Ha Thuy Long<sup>4</sup>.

<sup>1</sup>INRNE - Bulgarian Academy of Sciences, 72 Tzarigradsko chaussee, blvd.-1784 Sofia, Bulgaria.

<sup>2</sup>IPN-Orsay, CNRS-IN2P3 Universit Paris XI, 15 rue Georges Clémenceau F-91406 Orsay France.

<sup>3</sup>CENBG CNRS IN2P3-Universit Bordeaux I, F-33175 Gradignan cedex France.

<sup>4</sup>Vietnam National University at Hanoi, 334 Nguyen Trai, Hanoi, Vietnam.

**Abstract.** Within the Higher Tamm-Dancoff Approximation (HTDA), single particle states associated with a mean field of the Hartree-Fock type are used into shell model like calculations. Recently, this approach has been used for ground state calculations in magic nuclei and in the  $N = Z$  mass region, as well as to study properties of some important isomeric states. The Cranking version of this formalism (Cr. HTDA) represents an attempt to reproduce rotational bands up to high spins in heavy nuclei. In this context, through the use of the mean field part of HTDA, many deformation and rotation effects (as intruder orbitals and effects of the time reversal symmetry breaking) are included in the configuration space. This work discusses the Cr. HTDA results obtained for two *Pb* isotopes (in order to test the approach), when using up to 2 particles - 2 holes excitations and provides tests for enlargement of the configuration space by 4 particle - 4 holes excitations. It is focused on the configuration space properties, improvement of truncation schemes, computational problems and saturation behavior of some physical quantities.

## 1. Introduction

The study of nuclear structure, when using effective phenomenological nucleon-nucleon forces is a well developed theoretical approach and has already given many and impressive experimentally verified results. When using microscopic approaches, nuclear phenomena could be described quite precisely with significant predictive power. The combination of microscopic approach and effective phenomenological nucleon-nucleon interactions allows to model nucleus behavior in mostly any state. As far as, superdeformed bands represent an example of two extremes: extreme in deformation and in some cases extreme in very high spin, they are suitable for test of modelling theories. Such extreme states allow stretching the theoretical approaches to their limits. As such a test, one studies in this article the present performance of the cranked Higher Tamm-Dancoff Approximation (Cr. HTDA) theory in a domain, where Cr. HFB studies already show at the same time important successes, as well as some deficiency related to non-exact conservation of the particle number.

The HTDA theory, was described and developed in Ref. [1, 2] and used in some specific cases [3, 4, 5, 6] of nuclear phenomena. The specific use for rotational bands description is hindered by exceptional strong configuration space requirements, in the domain of superdeformed heavy nuclei, where a lot of Cr. HFB ([7, 8, 9, 10, 11] or Cr. RHB [12] calculations were performed.

Nevertheless, such an approach represents a unique possibility to test effective phenomenological nucleon-nucleon forces when particle number is treated exactly and in a natural way does not allow spurious transition phenomena.

Without using projection methods, the Cr. HTDA could avoid configuration mixing between neighboring nuclei and thus could describe some fine shell structure driven phenomena as band crossings or band terminations. Nevertheless, a configuration space of sufficient size is required. We will discuss here some conditions able to assess the space size adapted to the problem. The testing calculations presented here concern two *Pb* isotopes -  $^{192}\text{Pb}$  and  $^{194}\text{Pb}$ .

## 2. The Cr. HTDA essentials

The HTDA method, has been fully described in Ref. [1, 2]. Let us recall the three main steps upon which it relies and some particularities of the interactions used in the current study:

i) A  $n$ -particle - $n$  hole Slater determinant basis set is built on a Hartree-Fock "vacuum" solution associated with the one-body density matrix  $\rho^0$  and the corresponding selfconsistent HF Hamiltonian  $h^0(\rho^0)$ . In the present work, this mean field is built on the ground of the Skyrme SkM\* parametrization of the effective Skyrme nucleon-nucleon interaction [13].

ii) To mock the exact residual interaction we consider a  $\delta$  pairing interaction and deducing its contributions of the "mean field" type leads us to the residual interaction  $V_0^{res}$  and therefore to the Hamiltonian  $H_0^{HTDA} = h^0(\rho^0) + V_0^{res}$ . The corresponding stationary Schroedinger equation is solved. In practice, only the state with the lowest energy is of physical interest here, (namely  $\Psi$ ). It is extracted using standard Lanczos algorithm and formally writes :

$$|\Psi_0\rangle = |\phi_0\rangle + \sum_{i=\forall 1p1h} \chi_1^i |\phi_1^i\rangle + \sum_{j=\forall 2p2h} \chi_2^j |\phi_2^j\rangle + \sum_{k=\forall 3p3h} \chi_3^k |\phi_3^k\rangle + \dots, \quad (1)$$

where the many-body ground-state wave-function is described by the Slater determinant  $|\phi_0\rangle$  built with the neutron or proton lowest energy single particle (sp) states. When promoting a nucleon from a hole state  $\varphi_a$  to a particle state  $\varphi'_a$  neglecting the mean-field changes, one gets a new determinant  $|\phi_1^i\rangle$  which corresponds to the particular 1 particle -1 hole excitation (1p1h) associated with the exchange of  $\varphi_a$  by  $\varphi'_a$ . In this way, one built the many-body basis of Slater determinants  $|\phi_2^j\rangle$ ,  $|\phi_3^k\rangle$  ..., corresponding to 2 particles -2 holes (2p2h), 3 particles -3 holes (3p3h) ... excitations of the reference quasivacuum Slater determinant  $|\phi_0\rangle$ . Within this space, the  $N$  (or  $Z$ ) body wavefunction is finally represented by the expansion coefficients  $\chi_n^m$ . The basis of Slater determinant  $|\phi_n^m\rangle$  is of course infinite and has to be truncated to be handled by computers. That point will be discussed in the next chapters. Note that here, like in most HFB or HF plus BCS calculations, the considered excitations do not mix different charge states.

iii) From the correlated wavefunction  $\Psi_{\alpha=0}$  written as the combination of Slater determinants Eq. (1), one deduces a new one-body density :

$$(\rho_{\alpha=1}^{corr})_{ij} = \langle \Psi_{\alpha=0} | a_j^\dagger a_i | \Psi_{\alpha=0} \rangle \quad (2)$$

which defines through Skyrme functional a new one body Hamiltonian  $h^0(\rho_{\alpha=1}^{corr})$ , whose solutions define a new set of  $n$  particle -  $n$  hole states (step i). The HTDA Hamiltonian writes in this new space  $H_{\alpha=1}^{HTDA} = h^0(\rho_{\alpha=1}^{corr}) + V_{\alpha=1}^{res}$  from which the new correlated wave function (step ii) is extracted as  $\Psi_{\alpha=1}$ , the process being pursued increasing the index  $\alpha$  up to convergence with requirements for the lowest energy or for the decomposition numbers  $\chi_n^j$  of the wave function  $\Psi$ .

### 2.1. The Cranked HTDA Hamiltonian

These basic principles have been kept in the present routhian approach, in which a linear constraint on the component  $J_x$  of the angular momentum is added, writing therefore:

$$\hat{H} = \hat{H}_{Skyrme} + \hat{H}_{Coulomb} + \hat{H}_{pair} - \Omega \hat{J}_x \quad (3)$$

where  $\hat{H}_{pair}$  is a zero-range volume  $\delta$  pairing interaction, and where  $\Omega$  is the angular velocity i.e. the Lagrange multiplier associated with the dynamical constraint  $\hat{J}_x$  - the x-axis component of the angular momentum.

Equation (1) is used to write the HTDA Hamiltonian matrix of in the  $nph$  representation :

$$H_{ij} = \langle nPh_i | \hat{H} | mPh_j \rangle = \langle \phi_n^i | \hat{H} | \phi_m^j \rangle = \begin{pmatrix} 0P0H & 1P1H & 2P2H & \dots \\ 0P0H & H_{00} & H_{01} & H_{02} & \dots \\ 1P1H & H_{10} & H_{11} & H_{12} & \dots \\ 2P2H & H_{20} & H_{21} & H_{22} & \dots \\ \dots & \dots & \dots & \dots & \dots \end{pmatrix} \quad (4)$$

One neglects the small polarization changes of the mean field caused by the  $nph$  excitations, when  $n$  is a small number. This is done in analogy with the Koopmans approximations used for odd systems. Thus, mean field contributions vanish in the non diagonal terms of (4). The non-diagonal matrix elements are only due to the residual interaction defined as :

$$\hat{V}^{res} = \hat{V} - \hat{V}_{HF}, \quad (5)$$

where  $\hat{V}$  is the two-body interaction including all interactions and  $\hat{V}_{HF}$  is the one-body reduction of the Skyrme and Coulomb interactions. The non-diagonal matrix elements of  $\hat{H}$  are thus given by :

$$H_{ij} = \langle \phi_n^i | \hat{V}^{res} | \phi_m^j \rangle. \quad (6)$$

The only terms which are due to the mean field belong to the diagonal matrix elements  $H_{ii}$  which are written as:

$$\langle \phi_n^i | \hat{H}_{Skyrme} + \hat{H}_{Coulomb} - \Omega \hat{J}_x | \phi_n^j \rangle = H_{00} + \delta_{ij} \left( \sum_p e_p^i - \sum_h e_h^i \right) \quad (7)$$

Here  $e_h$  and  $e_p$  are the energies of the hole and particle sp-states defining  $\phi_n^i$  and  $H_{00} = \langle \phi_0 | K + V_{HF} | \phi_0 \rangle$  is the total energy of the quasivacuum Slater determinant.

### 2.2. The zero-range pairing force

In general in both channels - particle-hole or particle-particle, one could use the same interaction or different ones, but it is difficult to find at this stage of the research, a computationally doable approach with realistic interactions which works on both channels. Therefore, in this study one uses a volume zero-range pairing force as residual interaction (Ref. [14]) - similar to that employed in static HTDA calculation of Ref. [1, 2]), limited to act only on the states whose energies are in the vicinity of the Fermi energy  $\lambda$ . To avoid any artificial sharp cutoff energy dependence (due to the appearance or disappearance of some single particle state into the window upon varying any continuous parameter like  $\Omega$ ), it is customary to introduce a smoothing factor  $f(e_i)$  defined by a cutoff parameter  $X$  (in the present case  $X = 4MeV$ ) and a smoothing parameter  $\mu$  (here,  $\mu = 0.5MeV$ ) and written as :

$$f^2(e_i) = \frac{\left(1 + \exp\left(-\frac{X}{\mu}\right)\right)}{\left(1 + \exp\left(\frac{(e_i - \lambda) - X}{\mu}\right)\right)}. \quad (8)$$

The matrix element of the interaction takes then the form:

$$\tilde{V}_{ijkl}^{pair} = V_0 \left\langle ij \left| \frac{1 - \vec{\sigma}_1 \cdot \vec{\sigma}_2}{4} \delta(\vec{r}_1 - \vec{r}_2) \right| \tilde{kl} \right\rangle f(e_i) f(e_j) f(e_k) f(e_l), \quad (9)$$

where  $V_0$  is the pairing strength for a given isospin, and where  $\sigma_i$  are the usual Pauli matrices. Finally,  $V_0$  values will be discussed hereafter in section 4. We take into account only the sp-states whose Hartree-Fock energies belong to the window:

$$\lambda - (X + 5\mu/2) < e_i < \lambda + (X + 5\mu/2), \quad (10)$$

where  $\lambda$  stands for the Fermi energy.

### 3. Symmetries

Similarly to Ref. [8, 15] we preserve the parity and signature symmetries in the HF cranking Hamiltonian. The corresponding sp-spectrum (and the  $n$  particles -  $n$  holes deduced Slater determinants) are also parity-signature symmetric. The selection rules for the zero-range volume pairing interaction when using sp-states with good parity-signature symmetries are such that:

$$V_{ijkl}^{pair} = 0, \text{ when, } s_i s_j s_k s_l \neq 1 \text{ or } \pi_i \pi_j \pi_k \pi_l \neq 1,$$

where  $s_i, s_j, s_k, s_l$  and  $\pi_i, \pi_j, \pi_k, \pi_l$  are signatures and parities of the sp states with indexes  $i, j, k$ , and  $l$  respectively.

When taking these rules into account, it is straightforward to verify through the Wick's theorem from Eqs. (6), (7) and (9), that the Hamiltonian matrix become block-diagonal in four blocks of states, corresponding to the four possible couples of parity and signature values. This allows us to diagonalize separately in four blocks for each isospin. Of course, the final result to be considered will lie in the block which gives the lowest total energy  $\langle \hat{H} \rangle = \langle \Psi | \hat{H} | \Psi \rangle$ . Similarly, the sp-density matrix is also block diagonal and hence one performs the routhian calculations separately each block.

### 4. Truncations and parametrization of the force

In such a shell-model like problem, the corner stone is clearly to determine the size of the  $npnh$  basis which will give a convincing accuracy and convergence of solutions. This depends on the the size of the restricted sp-space for the pairing force action, on the rank of excitations included in the configuration space and, an eventual energy cut-off of the configurations of a given rank. Some important remarks can be made in order to determine the "sufficient" conditions for convenient and still tractable size of the basis. Upon increasing the configuration space, one must study the trend of some important physical quantities which "saturate", which may be interpreted as an indication that this configuration space is not enough. Further, considerations over convergence and boundary conditions for such quantities must be taken into account in order to determine the right recipe for basis truncations and the parametrization of the residual interaction.

Here, one is concerned by the reproduction of the pairing properties of superdeformed rotational bands in the  $A = 190$  mass region. In general, one can adjust the pairing strength parameters  $V_0$  for neutrons and protons (named here  $V_n$  and  $V_p$ ) in order to obtain meaningful

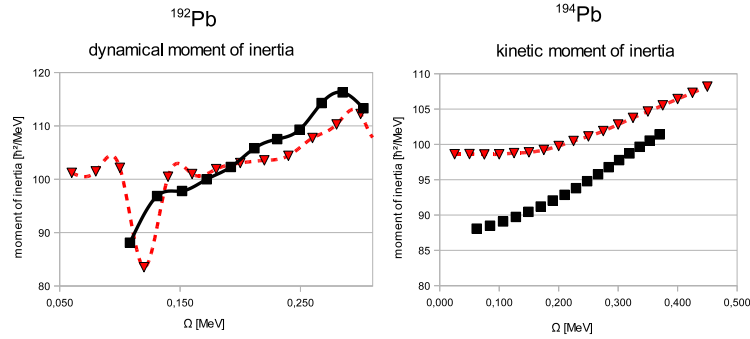


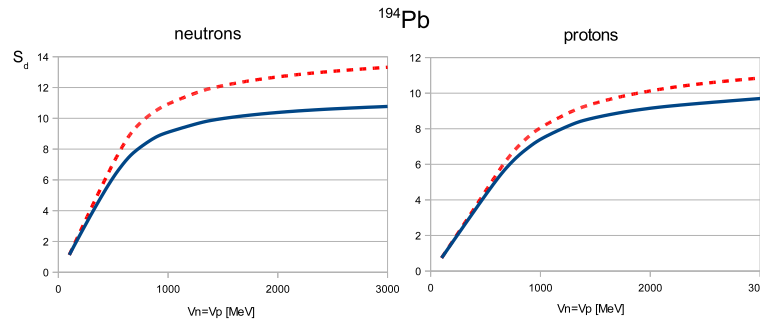
**Figure 1.** HTDA dynamical moments of inertia of  $^{192}\text{Pb}$  (red, triangles), HTDA kinetic moments of inertia of  $^{194}\text{Pb}$  (red, dashed line, triangles), experimental values (squares) versus angular velocity.

values for the kinetic moment of inertia at low angular velocities. But, when vibrational modes are not explicitly included in the formalism, one must subtract about 15% of such a value in order to obtain the experimentally deduced moments of inertia when taking them into account considerations (see Ref. [16]) for vibrational collectivity. For simplicity, everywhere in this study, one consider  $V_n = V_p$ , but computations for non-equal  $V_n$  and  $V_p$  have been also performed [17].

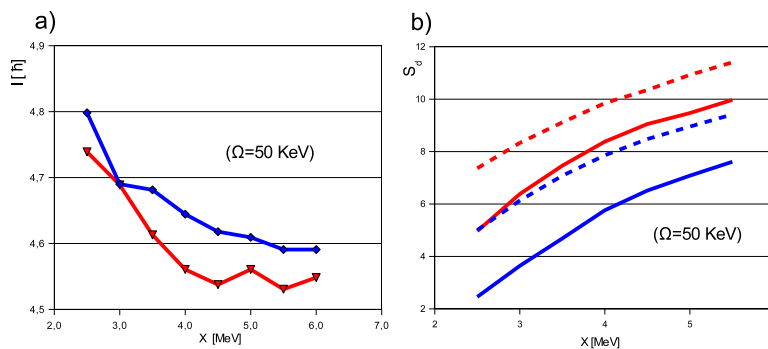
Figure 1 displays the Cr. HTDA results for the  $^{192}\text{Pb}$  Yrast SD band kinetic moments of inertia, compared to the data, using the following truncation conditions: only 0p0h, 1p1h and 2p2h excitations are included in the configuration space, their energy is restricted to be below  $2X + 5\mu/2$  value. Although, good convergence is obtained, an important band crossing at low angular momentum is reproduced and the band termination is also in accord with the data; the slope of the moment of inertia is too weak and one could imagine that such phenomenon is related with the size of the truncated configuration space. The same is true for the slope of the kinetic moment of inertia of SD-1 band of the  $^{194}\text{Pb}$  isotope. In order to understand the reason for the weak slopes, one tests first the response of the system, when changing the pairing interaction strength within large boundaries. It is given on figure 3 for the  $^{194}\text{Pb}$  Yrast SD band, where a measure of spreading ( $S_d$ ) of the occupation numbers around the Fermi level, defined by  $S_d = \text{tr}(\hat{\rho}(1 - \hat{\rho}))^{1/2}$  (which is equivalent in the BCS notation to  $S_d = \sum_i (u_i v_i)$ , see e.g. Ref. [17]) is plotted against the pairing strength.

Figure 2 displays the Cr. HTDA results as obtained from static calculations ( $\Omega = 0$ ). When  $S_d \rightarrow 0$  then one is performing Cr. HTDA without correlations. When one increases the pairing strength the amount of correlations (measured by  $S_d$ ) gradually increases, upon arriving at some level, where it tends to increase only marginally. Something limits its further expansion. It is our contentio that this limits its further expansion. One supposes that this is due to the restricted character of the configuration space. As a matter of fact, it is limited in terms of energy and rank of the p-h excitations.

On figure 3, at low angular velocity ( $\Omega = 50\text{KeV}$ ), one shows the progression of the angular momentum versus the change of  $X$ . When  $X \rightarrow 0$  one must clearly obtain the Cr. HF limit. Upon increasing the cut-off parameter, the pairing correlation effects are increasing and are expressed also by increasing. This may be expressed also as an increase of counter-rotating intrinsic currents (see Ref. [18, 19]) and thus they gradually decrease the angular momentum, the kinetic moment of inertia and minimize the collective kinetic rotational energy for a given angular velocity. Some shell effects related to the nature of new included sp-states in the



**Figure 2.** Spreading of the occupation numbers around the Fermi level ( $S_d$ , dimensionless) versus pairing strength  $V_n = V_p$  (in  $MeV$ ). The blue continuous line corresponds to Cr. HTDA calculations for up to 2p2h excitations, the red dashed - adds highly truncated (as described in the body text) version of the 4p4h space.



**Figure 3.** Angular momentum  $I$  - (side a) and spreading  $S_d$  - (side b) around the Fermi level versus the cut-off parameter  $X$ . Red curves and full triangles on side a (resp. blue curves and diamonds on side (a)) stands for  $V_n = V_p = 1400 MeV$  (resp.  $V_n = V_p = 700 MeV$ ). On side (b) full lines (resp. dashed lines) indicate proton (resp. neutron) distribution.

window could change slightly the smoothness of such progression, but not the trend. When one increases too much the pairing interaction window, the intrinsic vortical current generation begins to saturate and the shell effects could even counter the decreasing trend as it is shown at this figure for higher  $X$ . This behaviour on figure 3 is more pronounced for the curve with the larger value of the pairing strength  $V_n = V_p = 1400 MeV$  as compared with  $V_n = V_p = 700 MeV$ , because when  $X = 4 MeV$  such a pairing strength already lies deep in the saturation zone as seen on figure 2. As far as, the type of excitations is limited to 2p2h, one is unable to obtain less saturated curves, especially using pairing strengths, suitable to reproduce the experimental  $I$ . As an example, for  $X = 4 MeV$  and  $\mu = 0.5 MeV$ , one must choose a very high pairing strength ( $1400 MeV$ ) in order to obtain meaningful value of  $I$  at low spin. Then, the only way to get pairing strengths, which at the same time correspond to non-saturated stretches of the curves on figure 2 and give the right  $I$ , is to increase the rank of excitations included in the configuration space. Especially interesting is the addition of 4p4h excitations to the configuration space, because when the residual interaction favors pairing correlations, the excitations of pair rank

represent biggest share in the wave function decomposition mix in equation 1. On figure 2 one has also reported the change, produced over the spreading ( $S_d$ ) by adding 4p4h excitations under a special selection/truncation scheme discussed below. As it is seen from figure 2 the addition of 4p4h excitations allows to obtain the the same amount that with  $V_n = V_p = 1400 MeV$ , but with lower values of pairing strength. This time, a range of  $V_n = V_p$  between 900 and 1000 MeV is sufficient to achieve the same amount of correlations (and spin). That is mostly out of the saturation zone. When computational difficulties will be resolved as discussed below, one will include more 4p4h and possibly all of the 3p3h excitations in the configuration space and thus one will obtain realistic pairing strengths probably far below the saturation region. At the limit of a full configuration space one would obtain pairing strengths very close to the BCS ones.

The recipe to select the most "important" 4p4h excitations included in the space of the present calculations is described below. At any Cr. HTDA iteration with 0p0h, 1p1h, 2p2h, 4p4h excitations a faster and preliminary iteration with only up to 2p2h excitations is performed, where the 200 2p2h excitations with highest probability ( $\chi^2$ ) in the decomposition (1) are isolated. Next, the genuine Cr. HTDA iteration with 0p0h, 1p1h, 2p2h, 4p4h excitations is performed, where the 4p4h excitations used are only those, which are based on the selected 200 high probable 2p2h excitations. This is done by exciting 2 more particles and holes on these particular configurations. They are moreover limited in energy to up to  $2X + 5\mu/2$  energy level, which is the same as those for the 2p2h configurations and it is in agreement with the definition of the sp-window. In principle, the bulk of 4p4h excitations lies above this limit, but the computational limits restrict us to such schemes.

As already said, to extract a few eigenstates and eigenvalues in such matrices, the Lanczos algorithm has been used with the numerical code written by B.N. Parlett and D.S. Scott [20] available as an open source.

## 5. Computational background

A good computing speed is requested to be able to use an appropriate configuration space. The difference from existing large scale shell model calculations is that the configuration space could be smaller in our case, due to the fact that for stable heavy nuclei  $N > Z$ . One could, thus, neglect neutron-proton pairing correlations as already mentioned. But, by imposing meaningful value for the pairing interaction window -  $X = 4 MeV$  and  $\mu = 0.5 MeV$  one could obtain up to 60 sp-states in the so-defined "valence" space for one nucleon type. This exceeds by far the usual large shell model valence space numbers, where Wick theorem are performed for much more restricted spaces. In such Cr. HTDA window, only parity-signature symmetries are imposed and thus configuration space for up to  $10^6 - 10^7$  could be obtained. Here, the problem with the computation time does not lie in the Lanczos procedure process, as it is the case for large scale shell model calculations. In the Cr. HTDA method, the dimension of the energy matrix  $n$  is smaller, and eigenvectors for matrices of corresponding dimension could be easily found, taking into account their sparse nature, in a Lanczos algorithm. Here, the time for building the matrix is critical, as far as many Wick theorem calculations must be performed quickly (about  $10^{12} - 10^{14}$  times) when Hamiltonian is changed at any iteration. Such problem could be solved by identifying and thus excluding quickly the non-zero elements of  $H_{ij}$ . On figure 4 the dependence of time of matrix construction and eigen value finding is displayed as a function of the size of the matrix  $n$ .

One uses in our case a binary description of any excitation, as an up to 64-bit bitstring is assigned to describe the particle part of any type of excitation and another 64-bit bitstring for the hole part of the excitation. For example the excitation defined below on the left side:

$$|A \rangle = a_{i_1}^+ a_{i_2}^+ a_{i_3} a_{i_3} |H F core \rangle \rightarrow \{(00001000010000)_{particles}, (0000000100100)_{holes}\}, \quad (11)$$



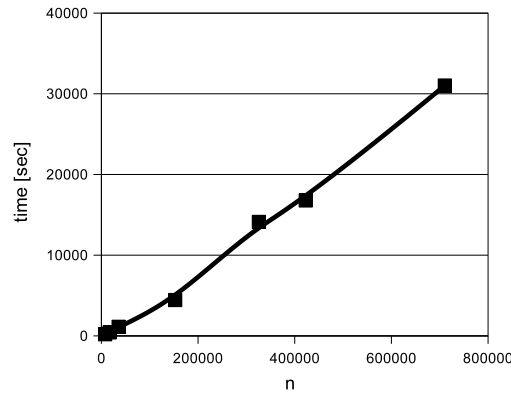


**Figure 4.** The time necessary to build the matrix and find the lowest eigensolution versus different dimensions ( $n$ ) of the matrix

is represented by the couple of bitstrings on right. Here, any bit set to 1 represents a specific particle or hole sp state excited in the considered configuration. The bits corresponding to other sp states are set to 0. In such a way excitations in a pairing action window of up to 128 sp-states could be described. Let us consider matrix elements of equation (6) of the type

$$\sum_{ijkl} V_{ijkl} \langle HFcore | a_{i_1}^+ a_{i_2}^+ \dots a_{i_{n+1}} a_{i_{n+2}} \dots | a_i^+ a_j^+ a_l a_k | a_{j_1}^+ a_{j_2}^+ \dots a_{j_{n+1}} a_{j_{n+2}} \dots | HFcore \rangle \quad (12)$$

A 2-body operator can change only 4 states/bits of the description of the right quantum state. The Hamming distance between two bitstrings representing the states  $|A\rangle$  and  $|B\rangle$  is defined as the sum of the numbers of particle and hole excitations necessary to transform one state into the other. This allows us to write in simple terms the selection rules for having non vanishing matrix elements for a  $p$ -body interaction : the Hamming distance between the l.h.s and the r.h.s of the matrix element should be less than  $2p$ . For example, if one looks for  $\langle A | V^{res} | B \rangle$  calculation, where  $|A\rangle$  is described by the couple of bitstrings in Eq. (11) and  $|B\rangle$  for instance as:

$$|B\rangle = a_{j_1}^+ a_{j_2}^+ a_{j_3} a_{j_3} | HFcore \rangle \rightarrow \{(00000000000011)_{particles}, (0001100000000)_{holes}\}, \quad (13)$$

then the bitwise exclusive (XOR) operation between bitstrings, which describe  $|A\rangle$  and  $|B\rangle$  gives:

$$\{(00001000010011)_{particles}, (0001100100100)_{holes}\}, \quad (14)$$

where the ones take places of sp-excited states which differ in  $|A\rangle$  and  $|B\rangle$ . In this particular case, one sees that  $|A\rangle$  and  $|B\rangle$  differ by 8 excitations and thus it requires at least a 4-body  $V^{res}$  operator. Then one can simply skip the calculation of this matrix element and go the next. The faster the Hamming distance computation is, the faster the  $H_{ij}$  construction becomes and less truncation limits of the configuration space are needed for a given total computing time. One uses, here, the Donald Knuth algorithm (Ref. [21]) for quick finding the Hamming distance for any  $i$  and  $j > i$  (the  $H_{ij}$  matrix is symmetric and real) which could in principle compute one Hamming distance for 10-60 clock cycles, when one programs it in a high level language. But, recently the NSA of US obliged indirectly microprocessors vendors to add to

mass market microprocessor's instruction sets (used so frequently in NSA supercomputers), instructions that allow hardware realizations of Hamming distance calculation for bitsets. These SIMD instructions (instruction POPCNT in the SSE4a instruction set of the x86 processors) allow assessing 30 bitstrings per clock cycle, thus promising much higher speed of calculation of our matrix elements. Using them together with other similar techniques of calculations, the inclusion of all 3p3h and 4p4h excitations into our configuration space should be possible. It is expected that such an enlargement of our configuration mixing basis should be able to cure the deficiencies of the moments of inertia slopes obtained up to now with the Cr. HTDA method.

## 6. Conclusions and perspectives

The Cr. HTDA calculations, when performed with sufficiently large configuration spaces and less truncations, should constitute a powerful tool to study theoretically rotational bands. In the same framework, pairing or (low multipolarity) multipole-multipole forces could be taken into account. Such task requires some advanced computational techniques. When applied, they are expected to yield improved results for rotational or mixed vibrational-rotational bands. It has been the object of this contribution to explore the potential consequences of using such techniques to describe these bands.

## Acknowledgements

One of authors was supported by contract F-1502/05 of Bulgarian NSF in order to achieve part of the work and to participate in the Varna Nuclear Physics school. Three of us were supported also by PICS agreement 4847 (2009) CNRS-IN2P3/BAS.

## References

- [1] Pillet N, Quentin P and Libert J 2002 *Nucl. Phys. A* **697** 141.
- [2] Pillet N, PhD Thesis 2000, Université Bordeaux I, France.
- [3] Ha T L, Ph. D. Thesis 2004 Université Bordeaux I, France.
- [4] Pillet N, Berger J-F and Caurier E 2008 *Phys. Rev. C* **78**, 024305
- [5] Bonneau L, Quentin P and Sieja K 2007 *Phys. Rev. C* **76**, 014304
- [6] Naidja H, Ph. D. Thesis 2009 Universit Sciences et Technologies - Bordeaux I
- [7] Terasaki J, Heenen P-H, Dobaczewski P and Flocard H 1995 *Nucl. Phys. A* **593** 1.
- [8] Gall B, Bonche P, Dobaczewski J et al. 1994 *Z. Phys. A* **348** 183.
- [9] Peru S, PHD thesis 1997 Université Paris VII France.
- [10] Bender M, Bonche P, Duguet T and Heenen P-H 2004 *Phys. Rev. C* **69**, 064303
- [11] Valor A, Egido J L and Robledo L M 1997 *Phys. Lett. B* **393** 249.
- [12] Afanasjev A V, König J and Ring P 1999 *Phys. Rev. C* **60** 051303.
- [13] Bartel J, Quentin P, Brack M, Guet C and Haakansson H B 1982 *Nucl. Phys. A* **386** 79.
- [14] Krieger S J, Bonche P, Flocard H and Quentin P 1990 *Nucl. Phys. A* **517** 275.
- [15] Goodman A L 1974 *Nucl. Phys. A* **265** 466.
- [16] Libert J, Girod M and Delaroche J-P 1999 *Phys. Rev. C* **60** 054301.
- [17] Libert J, Laftchiev H, Quentin P 2003 Contribution to 22nd International Workshop on Nuclear Theory, 16-21, Rila Mountains, Heron Press-Sofia
- [18] Durand M, Schuck P, Kunz J 1985 *Nucl. Phys. A* **439** 263
- [19] Laftchiev H, Samsen D, Quentin P and Mikhailov I N 2003 *Phys. Rev. C* **67** 014301.
- [20] Parlett B N and Scott D N 1979 *Math. Comp.* **217** 33-145.
- [21] Knuth D E, *The Art of Computer Programming*, Addison-Wesley Professional